FULL PAPERS

Magnetic Resonance in Medicine 50:936–943 (2003)

MR Spectroscopy of Muscle and Brain in Guanidinoacetate Methyltransferase (GAMT)-Deficient Mice: Validation of an Animal Model to Study Creatine Deficiency

W. Klaas Jan Renema,[1]* Andreas Schmidt,[2] Jack J.A. van Asten,[1] Frank Oerlemans,[3] Kurt Ullrich,[4] Bé Wieringa,[3] Dirk Isbrandt,[2] and Arend Heerschap[1]

As a model for guanidinoacetate methyltransferase (GAMT) deficiency in humans, a gene knockout mouse model was generated. Here we report on several metabolic abnormalities in these mice, observed by in vivo and in vitro MR spectroscopy. In ^{1}H MR spectra of brain and hindleg muscle a clearly reduced signal of creatine (Cr) was observed in GAMT-deficient (GAMT–/–) animals. Analysis of the ^{1}H MR spectra of GAMT–/– brain indicated little or no increase of a signal for guanidinoacetate (Gua). In proton MR spectra of muscle, a broad signal of low intensity was observed for Gua. However, substantial Gua accumulation in intact muscle tissue was unequivocally confirmed in high-resolution magic angle spinning spectra, in which the Gua signal was resolved as one clear sharp singlet. In ^{31}P MR analysis of brain and hindleg muscle a strongly reduced phosphocreatine (PCr) content was shown. In addition, a signal of phosphorylated Gua at 0.5 ppm upfield of PCr was observed, with much higher intensity in muscle than in brain. This signal decreased when ischemia was applied to the muscle and recovered after ischemia was released. Overall, the in vivo ^{31}P and ^{1}H MR spectroscopy of GAMT–/– mice is similar to that of human GAMT deficiency. This opens up new avenues for the fundamental study of tissue-type dependence of creatine synthesis and transport and for diagnostic and therapeutic aspects of creatine deficiencies in humans. Magn Reson Med 50: 936–943, 2003. © 2003 Wiley-Liss, Inc.

Key words: GAMT-knockout; energy-metabolism; creatine; magnetic resonance

Guanidinoacetate methyltransferase (GAMT) is a key enzyme in the biosynthesis of creatine (Cr), a process that mainly occurs in pancreas and liver (1). The first step on this synthetic route involves transfer of the amidino group of arginine to glycine, to yield ornithine and guanidinoacetate (Gua). Subsequently, GAMT facilitates the methylation of Gua to Cr.

Cr is a central compound in the energy metabolism of tissues such as muscle and brain. In these tissues it can be phosphorylated to phosphocreatine (PCr) using one of the five isoenzymes of creatine kinase (CK). Finally, Cr and PCr are catabolized to creatinine (Crn), which is excreted through the urine. To maintain a constant body pool of Cr, its breakdown and build-up via dietary intake and endogenous synthesis must be balanced and its transport across membranes of cells in various tissues must be tightly regulated (2).

GAMT deficiency was described for the first time as a new inborn error of metabolism (3) in an infant with extrapyramidal movement disorder, who had low Crn in serum and urine (3–6). To date, several cases of GAMT deficiency have been reported (7–11). Patients show symptoms in a wide range of severity (12) including developmental retardation (4,7–9,11), muscle hypotonia (3,5,8,11), extrapyramidal movement abnormalities (3–5,7), and epileptic seizures (7,8,11).

Localized MR spectroscopy (MRS) of the brain of young patients has played a decisive role in the elucidation of the pathophysiology of GAMT deficiency. A strongly reduced Cr signal was revealed by ^{1}H MRS (3,4,7–11,13). In ^{31}P MR spectra PCr was decreased and a new resonance appeared, which was assigned to phosphorylated Gua (PGua) (7,10,13). This assignment was confirmed by an additional resonance in the ^{1}H MR spectrum at 3.8 ppm, which is likely to arise from Gua protons (3,9,10,13).

Oral intake of arginine resulted in an increase of the Gua signal intensity in the proton MR spectra (3,13), while intake of Cr led to a partial restoration of the Cr signal (3,4,7,9–13), decrease of the Gua signal (3,7,10,13), and improvement of clinical symptoms (3–13).

To our knowledge, in only two patients with GAMT-deficiency was MRS of muscle performed. The first case study reported on a considerable signal for Cr in ^{1}H MR spectra of muscle but not in brain, and no peak at 3.8 ppm (10). In the ^{31}P MR spectrum only one peak was observed around 0 ppm, which was assigned to PCr. The second case study showed both PCr and PGua in ^{31}P MR spectra of muscle, while no ^{1}H Cr resonance was observed in brain (14).

[1]Department of Radiology, University Medical Center Nijmegen, Nijmegen, the Netherlands.

[2]Center for Molecular Neurobiology, University of Hamburg, Hamburg, Germany.

[3]Cell Biology, University Medical Center Nijmegen, Nijmegen, the Netherlands.

[4]Pediatric Hospital, University of Hamburg, Hamburg, Germany.

Grant sponsor: Deutsche Forschungsgemeinschaft; Grant number: SFB 545, Project A3 (to D.I. and K.U.); Grant sponsor: the Netherlands Organization for Scientific Research (NWO-ZONMW).

*Correspondence to: W.K.J. Renema, University Medical Center, Nijmegen, Dept. of Radiology, Geert Grooteplein 10, P.O. Box 9101, 6500 HB Nijmegen, The Netherlands. E-mail: k.renema@rad.umcn.nl

Received 9 January 2003; revised 12 May 2003; accepted 18 July 2003.

DOI 10.1002/mrm.10627

Published online in Wiley InterScience (www.interscience.wiley.com).

Detailed study of the pathophysiology of GAMT deficiency and possible treatment strategies is difficult in humans, as the disease is very rare. Therefore, GAMT-deficient knockout mice (GAMT–/–) were generated (15). This article presents the first results of ^{31}P and ^{1}H MRS of hindleg muscle and brain in these mice. The purpose of this work was to validate the GAMT–/– mice as a useful model for Cr deficiency in human patients and to initiate a study into tissue-type and dietary-composition dependent accumulation of Gua derivatives.

MATERIALS AND METHODS

Animals

GAMT–/– mice were generated by homologous recombination in embryonic stem cells (15). As a reference, heterozygous (+/–) and homozygous (+/+) wildtype-like (wt) littermates of the GAMT–/– animals were used. In previous studies (not published), Isbrandt et al. showed that no differences could be observed between these groups and that animals of both genotypes can serve as control. For the determination of the T_2 of water and methyl Cr protons in hindleg muscle, six wt-like mice with a randomly inbred mixed background of C57Bl/6 and 129/Ola were used.

During the MR experiments, all animals were anesthetized using 1% isoflurane in a gas mixture of 50% O_2 and 50% N_2O delivered through a facemask. Breathing frequency was monitored and a warm waterbed was used to keep the animals at normal body temperature. All experiments were approved by the local animal ethics committee.

MR Equipment

The in vivo MR experiments were performed on a 7.0 T magnet (Magnex Scientific, Abingdon, UK) interfaced to an S.M.I.S. spectrometer (Surrey Medical Systems, Surrey, UK) operating at 300.22 MHz for ^{1}H and at 121.53 MHz for ^{31}P. The horizontal magnet was equipped with a 150 mT/m shielded gradient set and had a free bore size of 120 mm.

High-resolution magic angle spinning (HRMAS) spectroscopy experiments were performed on muscular tissues using a Bruker DRX 500 MHz spectrometer.

MR Spectroscopy Studies

To get a good overview of the phenotype of the GAMT–/– mice, ^{1}H and ^{31}P MR spectroscopy studies of both hindleg muscle and of brain were performed. In the ^{1}H MR experiments Cr refers to the sum of Cr and PCr.

For the ^{1}H MR studies on the mouse brain, a 12 mm surface coil anatomically shaped for mouse brain was used. Additional perspex earbars provided stereotactic fixation. Localized spectroscopy was performed using a STEAM sequence (TE = 10 ms, TM = 15 ms, TR = 5000 ms, 64 averages) with VAPOR water suppression (16) and outer volume suppression. A $3 \times 3 \times 3$ mm^3 (27 μl) voxel was positioned in the center of the brain guided by gradient echo images. In this study, measurements were performed in seven GAMT–/– and five wt animals.

The ^{31}P MR brain measurements were done using two surface coils, tuned to the ^{31}P frequency and working in quadrature mode. A large ^{1}H surface coil was utilized for shimming, imaging, and localization. To prevent contamination with signal from the masseter muscles, an ISIS sequence (17) was used (TR = 7000 ms, 8 step phase cycle, 512 averages), consisting of a 6.5 kHz adiabatic hyperbolic secant pulse for inversion, together with a 50 μs rectangular 90° RF pulse for excitation. A voxel with size $6.5 \times 6.5 \times 4.5$ mm^3 (190 μl) was positioned in the brain guided by gradient echo images. The mouse head was fixated using the quadrature surface coil and earbars.

^{1}H MR measurements on the mouse hindleg were done using an Alderman-Grant type of coil (18), oriented at the magic angle (55°) with respect to the main magnetic field to reduce dipolar interactions (19). The same STEAM sequence was used as in the ^{1}H brain measurements (voxel size $1.8 \times 1.8 \times 3.4$ mm^3, TR = 5 sec, 128 averages). For absolute quantification, the T_2 for water and Cr protons was determined by acquiring a suppressed and water-suppressed ^{1}H spectra at six different echo times in a separate experiment.

^{31}P MR pulse acquire experiments (TR = 7000 ms, 64 averages) on the hindleg were done using a three-turn solenoid coil, together with a proton Alderman-Grant type of coil for shimming. ^{31}P MR experiments on hindleg muscle and brain and ^{1}H MR experiments on hindleg muscle were performed in seven GAMT–/– and seven wt animals.

Ischemic occlusion of skeletal muscle was applied to two GAMT–/– animals by clamping with a diaphragm plate, which allowed reversible and reproducible obstruction of blood flow through the hindlimb (20). ^{31}P MR spectra were obtained using a pulse-acquire sequence (TR = 1400 ms, 76 averages). After four reference spectra an ischemic period of 25 min was applied (14 spectra), followed by a recovery period of 16 min (9 spectra).

Three GAMT–/– and three wt animals were sacrificed and their hindleg muscles were removed and snapshot frozen in liquid nitrogen. The intact tissue was measured in a 12 μl rotor using HRMAS spectroscopy at 4°C with a spinning rate of 5 kHz. Residual rotor space was filled with a PBS-buffer/D_2O mixture (30/70). For 1D ^{1}H MR a CPMG pulse sequence was employed with a 90° pulse of 7.2 μs, while the time between the 180° pulses was one rotor period. Water was suppressed by presaturation and a T_2 filter of 50 ms was applied.

Chemical Analysis of Total Cr Pool

To serve as a reference to the ^{1}H MR spectroscopy brain metabolite values, the size of the total Cr pool (i.e., Cr plus PCr) was determined by chemical analysis. Five C57Bl/6 mice and five mice with a randomly inbred mixed background of C57Bl/6 and 129/Ola were sacrificed, after which their brains were snapshot frozen in liquid nitrogen. These frozen brains were crushed and extracted with 0.6 M $HClO_4$. The extracts were neutralized with 3 M KOH and the PCr and Cr were assayed via coupled enzymatic reactions (21). PCr and Cr concentrations were added to yield the total Cr pool size.

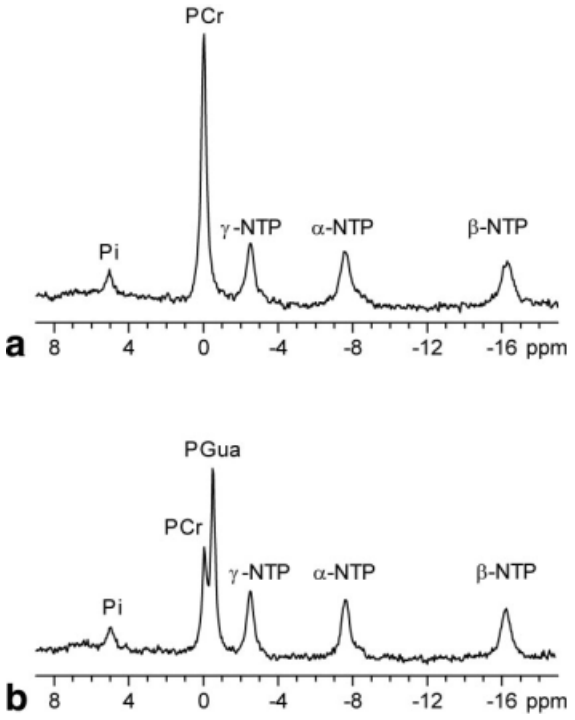

FIG. 1. ^{31}P MRS of hindleg muscle of wt (**a**) and GAMT–/– mice (**b**) in vivo. Peak assignments: inorganic phosphate (Pi); phosphocreatine (PCr); phosphorylated guanidinoacetate (PGua).

Data Processing

The ^{1}H MR data of brain were analyzed using the LCModel 5.2-2 software package (22). The unsuppressed water signal was used for eddy current correction, phasing, and normalization. The chemically determined Cr value was used to scale the MR determined metabolite values of the wt mice such that Cr values agreed. This scaling factor was also applied to the MR spectra of the GAMT mice, yielding absolute quantitative levels for all metabolites in the ^{1}H MR brain spectra.

The ^{31}P MR data of brain and muscle and the ^{1}H MR data of hindleg muscle were analyzed using the MRUI software package (23). In the data processing of ^{31}P MR brain spectra, the first-order phase was constrained. In GAMT–/– animals the damping of the PGua signal was set equal to the damping of the PCr signal. All signals were fitted assuming a Lorentzian line shape model function and normalized to the γ-NTP signal since the β-NTP signal was affected by a chemical shift artifact caused by the 6.5 kHz excitation pulse.

For the ^{1}H MR spectra of muscle, the first-order phase was constrained to zero because the first acquired data point was obtained at the top of the echo. Signals were eddy current-corrected using the unsuppressed water signal. The ratio of the linewidths of taurine and Cr was determined in wt animals. Cr linewidths were constrained to this ratio in both GAMT–/– and wt animals. All signals were fitted assuming a Gaussian line shape model function.

Absolute quantification of the Cr concentration in muscle was performed using the unsuppressed water signal. To correct for T_2 relaxation, the obtained water and methyl Cr spectra at six different echo times were fitted using MRUI (23) and the results at different echo times were fitted using a monoexponential curve. The proton signals in hindleg muscle are considered to be fully relaxed at a TR of 5 sec, and hence no T_1 corrections needed to be applied. Tissue water content was assumed to be 77% (24).

In the fitting procedure of the ^{31}P MR spectra data of hindleg muscle, the first-order phase was constrained. No other prior knowledge was used. Signals were fitted assuming a Lorentzian line shape model function and normalized to the β-NTP signal.

For brain and muscle, the pH was calculated from the shift in resonance position (S) of the inorganic phosphate (Pi) signal compared to the resonance position of PCr (25) using the equation $pH = 6.75 + \log((3.27\text{-}S)/(S\text{-}5.63))$.

A two-tailed Mann-Whitney test was used to test if GAMT–/– from wt metabolite levels were significantly different. Differences were considered significant at $P < 0.05$.

RESULTS

Muscle

The ^{31}P MR spectra of GAMT–/– animals showed striking differences with respect to wt spectra: PCr was significantly reduced and a new resonance appeared 0.5 ppm upfield of PCr (Fig. 1), which was assigned to PGua (13). Signal intensities of the residual PCr and newly formed PGua showed large fluctuations between animals. However, in all individual mice the ratio PGua/PCr was larger than 1, ranging from 1.4–8.8 (mean 3.4 ± 3). We observed that with higher PGua levels PCr levels tended to be equally lower; however, significance was not reached for this observation. Other metabolite levels (normalized to

Table 1
Ratios of Integral Values of Phosphorous Metabolite Signals and pH in Muscle and Brain

		PME/NTP	Pi/NTP	PCr/NTP	PGua/NTP	PGua/PCr	pH
Muscle*	wt	—	0.40 ± 0.06	2.66 ± 0.11	—	—	7.24 ± 0.09
	GAMT−/−	—	0.40 ± 0.08	0.76 ± 0.33	1.78 ± 0.42	3.4 ± 3	7.18 ± 0.06
Brain*	wt	1.09 ± 0.52	0.59 ± 0.16	1.36 ± 0.46	—	—	7.03 ± 0.08
	GAMT−/−	1.44 ± 0.74	0.71 ± 0.26	0.31 ± 0.10	0.28 ± 0.07	0.90 ± 0.2	7.11 ± 0.04

All values are presented as mean ± SD. PME: phosphomonoesters.
*Muscle metabolite signal values are normalized to the resonance of β-NTP, brain metabolite signals to γ-NTP (see Materials and Methods section for details).

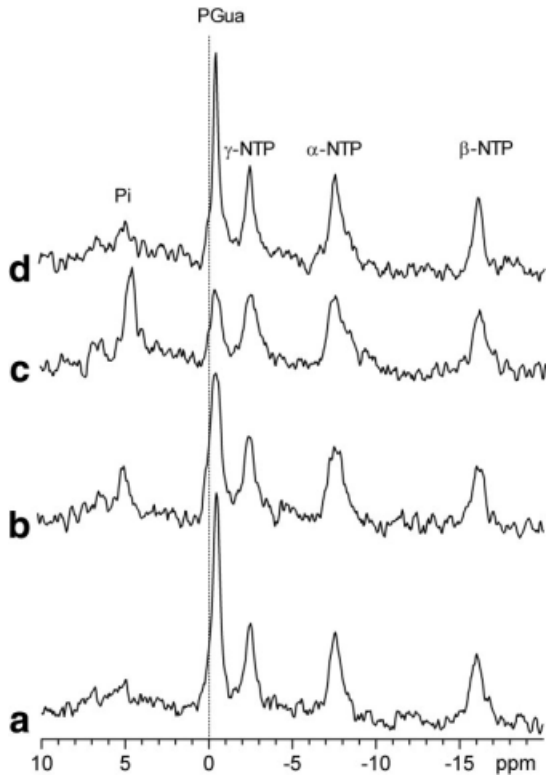

FIG. 2. In vivo ^{31}P MRS of hindleg muscle of GAMT-deficient mouse before (**a**) ischemia, after 5 min (**b**), and 25 min (**c**) of ischemia, and 5 min after releasing the ischemic clamp (**d**). A vertical line is positioned at 0 ppm to show that the large resonance is not PCr but PGua at −0.5 ppm.

the β-NTP signal) and tissue pH were not significantly different between GAMT–/– animals and their littermates (Table 1).

In order to find out whether PGua was metabolically active, ischemia of hindleg muscle was applied and monitored by ^{31}P MRS (Fig. 2). The spectrum before ischemia showed hardly any PCr signal, but a large PGua signal was apparent, especially in animals that were completely deprived of Cr. During ischemia the PGua signal decreased while Pi signals increased. After ischemia PGua increased again to its initial value. The time course of PGua depletion and recovery was of similar order as that of PCr in wt animals during and after ischemia (20).

The mono exponential fits of the water and Cr signals at different echo times yielded T_2 values for water and Cr proton spins of 21.9 ± 0.1 ms and 83 ± 4 ms, respectively. Those values were used to calculate absolute Cr concentrations.

Cr was significantly reduced in hindleg muscle of GAMT–/– animals (8.9 ± 3.8 mM) compared to wt animals (28.4 ± 2.6 mM) (Fig. 3). Despite the presence of PGua in the ^{31}P spectra, we observed hardly any signal for Gua in the ^{1}H MR spectra. Even though the spectra were obtained at the magic angle (55°) to reduce dipolar interactions, the Gua signal appeared at best as a broad line (Fig. 3c) in the spectra where Cr was largely reduced. It is of note that, although we did not explicitly study the relation between Cr content of the food and (P)Cr and PGua signals in muscle, the muscle ^{1}H MR spectrum showing largely reduced Cr (Fig. 3c) was taken in the same period, i.e., in mice eating the same batch of chow, as the ^{31}P MR spectrum, which shows hardly any PCr (Fig. 2a).

In an attempt to clarify the apparent discrepancy of the broad Gua signal, HRMAS experiments on muscular tissue of GAMT–/– and wt animals were performed (Fig. 4). This approach again yielded a clearly reduced Cr signal, but now at 3.78 ppm a clear signal for Gua appeared as a distinct singlet (Fig. 3c).

Brain

Next we used ^{1}H and ^{31}P MRS to establish whether the brains of GAMT–/– animals show the same metabolic features as brains of GAMT-deficient patients.

The chemical-determined values of the total Cr pool were 8.7 ± 1.0 and 8.6 ± 1.4 μmol/g wet weight for C56Bl/6 and mice with a randomly inbred mixed background of C57Bl/6 and 129/Ola, respectively. Using a brain density of 1.05 g/cm^3 (26), this could be converted to

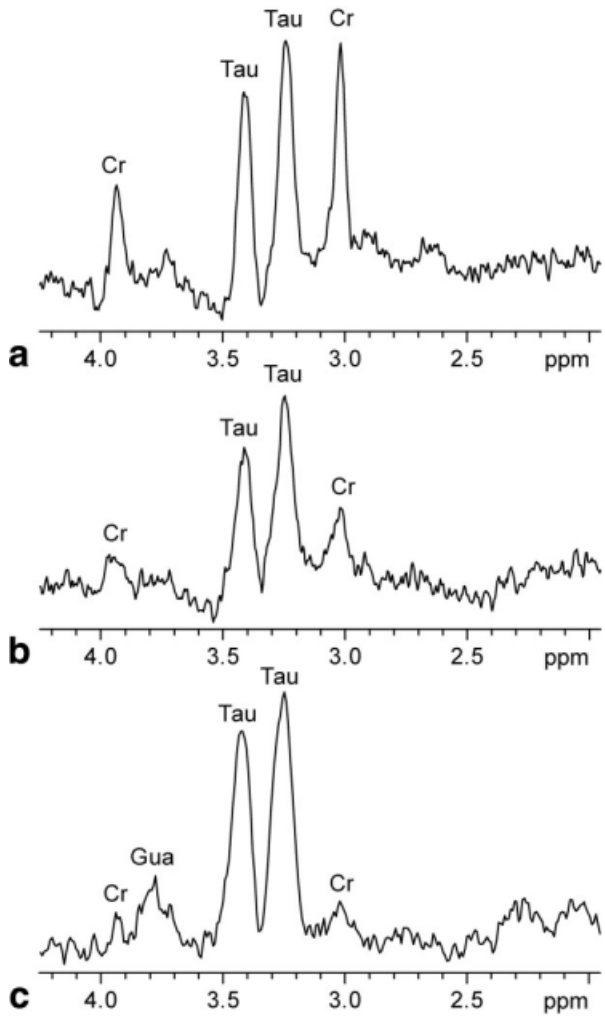

FIG. 3. Localized ^{1}H MRS of wt mice (**a**) and two GAMT–/– mice (**b,c**) hindleg muscle in vivo. Peak assignments: total creatine (Cr); taurine (Tau) guanidinoacetate (Gua). Gua is not observed in all GAMT–/– mice, only when Cr levels are very low (**c**).

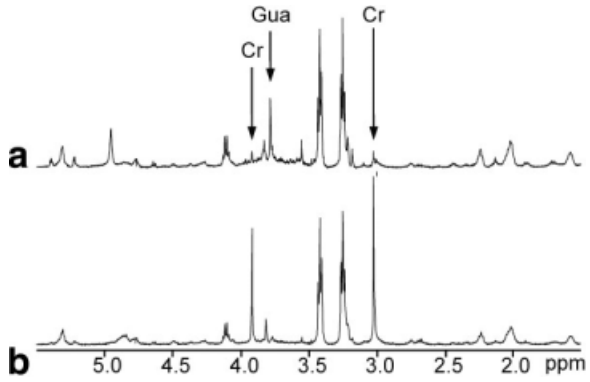

FIG. 4. Proton HRMAS MR spectra of intact GAMT–/– (**a**) and wt (**b**) muscle tissue in vitro. Peak assignments: methyl (3.0 ppm) and methylene (3.9 ppm) signals of total creatine (Cr); methylene signal of guanidinoacetate (Gua).

tissue concentrations of 8.3 ± 1.0 and 8.2 ± 1.3 mM, respectively.

Compared to wt, the Cr signal was significantly reduced in brain of GAMT–/– mice, although some broad signals remained present at 3.0 and 3.9 ppm (Fig. 5). No other metabolites analyzed from the ^{1}H MR brain spectra were significantly different between wt and GAMT–/– animals (Table 2). In addition, no significant increase could be observed at 3.8 ppm, where Gua resonates. Other metabolites resonate around this position and might obscure the Gua signal. However, in some wt and GAMT–/– animals there was a residual signal present at ~3.8 ppm after fitting the spectra. This residue was of low SNR and could not be quantified properly.

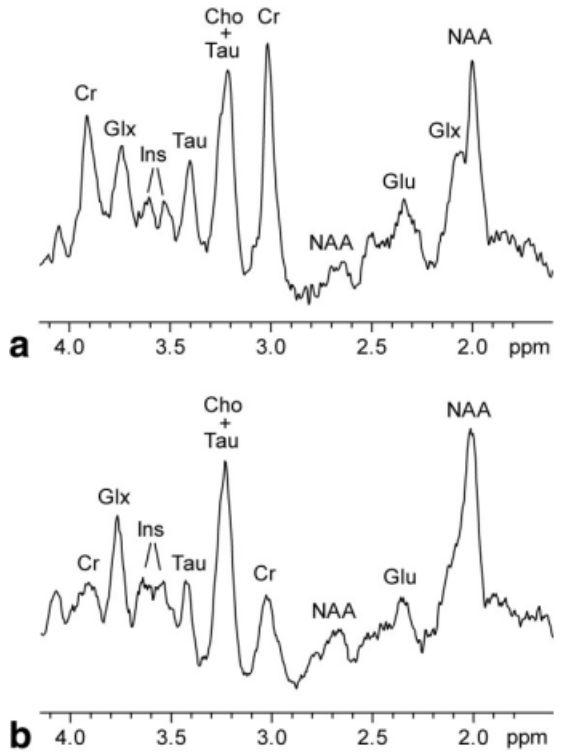

FIG. 5. Localized in vivo ^{1}H MR brain spectra of wt (**a**) and GAMT–/– (**b**) mice. Peak assignments: total creatine (Cr); choline (Cho); taurine (Tau); glutamate (Glu); glutamine and glutamate (Glx); myo-inositol (Ins); N-acetylaspartate (NAA).

Table 2
Tissue Concentrations of Brain Metabolites

	wt (mM)	GAMT−/− (mM)	Rat (mM) (16)
Taurine	5.8 ± 1.3	5.7 ± 1.6	6.0
Total choline[a]	1.9 ± 0.4	1.9 ± 0.4	0.5
NAA	5.3 ± 1.3	5.4 ± 0.8	8.9
Total creatine[b]	8.2 ± 1.2	1.4 ± 0.4[c]	8.5
Myo-inositol	2.2 ± 1.7	2.7 ± 0.9	4.4
Glutamate	3.9 ± 0.3	4.4 ± 0.6	8.3
Glutamine	1.8 ± 0.5	2.4 ± 0.7	2.7

All values are determined by ^{1}H MRS and scaled to biochemically determined Cr values (see Materials and Methods) and presented as mean ± SD.
[a]Phosphocholine + glycerol − phosphocholine.
[b]Creatine + phosphocreatine.
[c]Significantly different from wt ($P < 0.05$).

To see whether the residual Cr in GAMT–/– animals could result from intake via the mother milk of heterozygous mother animals, ^{1}H MR spectra of brain of GAMT–/– animals born to GAMT–/– mothers were also obtained. There was no distinction between ^{1}H MR spectra from GAMT–/– animals nourished by heterozygous or homozygous mutant females (data not shown), indicating that the genotype of the mother is not an important parameter for the metabolic profile of the offspring.

In ^{31}P MR spectra of the brain of GAMT–/– animals, a strongly reduced PCr signal was evident compared to the ^{31}P MR spectra of brain of wt animals (Fig. 6). In addition, a signal for PGua was observed 0.5 ppm upfield of PCr in GAMT–/– animals, at a much lower intensity than in muscle. The mean ratio of PGua/PCr in brain was smaller than 1 (0.9 ± 0.2). Other metabolite levels, normalized to γ-NTP, did not differ between GAMT–/– and wt animals in brain (Table 1).

DISCUSSION

In this study we showed that combined use of in vivo and in vitro MR spectroscopy is a valuable tool in elucidating the metabolic status of tissues of animal models for Cr deficiency. In combination with the introduction of the new GAMT knockout mouse model, this opens up many possibilities for studying the integral-physiological fate of precursors and products at various steps in the Cr-biosynthetic pathway, in much more detail than is possible in human patients.

MR Spectra of Brain and Muscle of GAMT-Deficient Mice

^{1}H MR spectra of both brain and muscle of GAMT–/– mice showed reduced levels compared to wt animals, but no complete absence of Cr. The Cr concentration in the food of the mice likely accounts for the continued presence of Cr.

There is evidence that the permeability of the blood–brain barrier for Cr is limited and that the brain partially relies on its own Cr synthesis (1,27,28). Therefore, it is

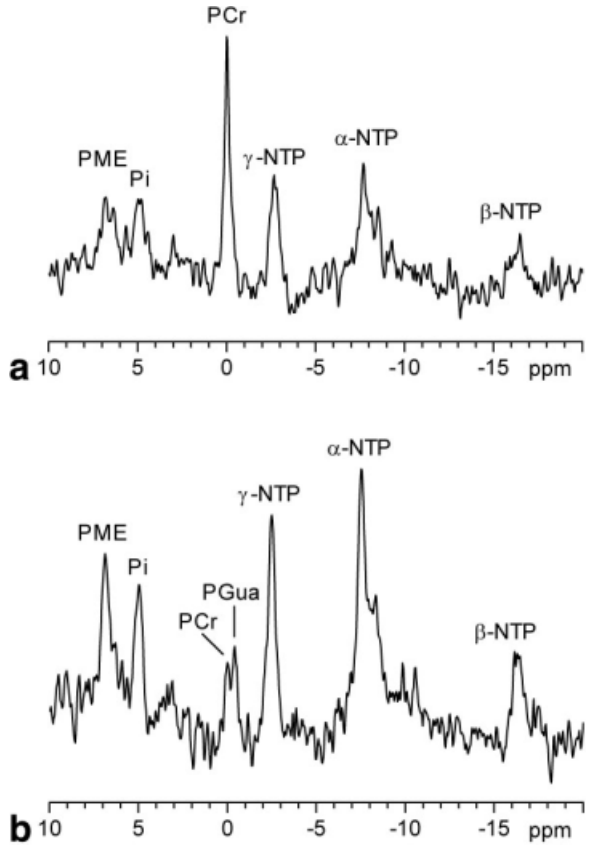

FIG. 6. Localized ^{31}P MRS of brain of wt (**a**) and GAMT–/– mice (**b**) in vivo. Peak assignments: phosphomonoesters (PME); inorganic phosphate (Pi); phosphocreatine (PCr); phosphorylated guanidinoacetate (PGua). Vertical scaling is arbitrary.

interesting to note that the reduction of Cr in GAMT–/– mice relative to the signal in wt animals appeared to be larger in brain than in muscle, which could be explained by a slower uptake of orally ingested Cr in the brain.

As absolute concentration data from proton MR spectroscopy of mouse brain metabolites have, to our knowledge, not been published, we compared our inferred values to metabolite concentrations measured in rat brain (16). Cr concentrations found in wt animals are almost similar to those found in rat. Strikingly, NAA and glutamate values are significantly lower in mouse brain than in rat brain. NAA is considered a neuronal marker (29) and the observed concentration is in agreement with other biochemical studies done in mice (29). The difference in rat and mouse NAA levels corresponds well with the factor of about 2-fold difference in cholinergic neurons per section of equal thickness in mouse and rat brain (30). Glutamate, important for synaptic signaling activity in brain, is stored mainly in neurons (31, and references therein), which explains the lower concentration found in mouse brain compared to rat brain. Although the concentration of choline compounds is in good agreement with values found in the human brain (32), it is higher than the concentration observed in rat brain. Why the concentration of choline compounds occurs at higher levels in mouse brain than in rat brain is currently not known.

A remarkable observation from MR spectra of GAMT–/– compared to wt was that the PGua content in muscle was much higher than in brain, although in brain we observed a more constant level of PGua and PCr. GAMT transcript and protein was found to be present in several normal human and mouse tissues, including in muscle at high levels (15). In muscle also, the enzyme AGAT, involved in synthesis of Gua, occurs at high levels (33). However, since the GAMT enzyme is lacking in GAMT–/– mice this does not necessarily mean that Gua will accumulate. Altered transport or change in feedback control of metabolic steps may also affect the rate of accumulation of precursors, and these factors may vary between tissues. Currently, we lack proper explanations for the differences in PGua and PCr levels between tissues. It has been suggested that brain is relatively self-sufficient in terms of Cr biosynthesis (34), whereas muscle is not. However, no data are available about the relative capacities of the different biosynthetic steps leading to the formation of Gua (and the conversion to Cr) or for the relative import capacities for Cr in different tissues. The permeability of the blood–brain barrier is suggested to be limited for Cr (1) and, throughout the brain, Cr transporters are not equally distributed. Cr uptake capacity almost surely differs between neural and glial cell types (28). In muscle fibers Cr transporters may be more equally distributed.

Visibility of Guanidinoacetate

If brain tissue ATP concentration is assumed to be ~3 mM (35) also in GAMT mice, PGua levels in brain can be estimated from the observed signal ratios (Table 1) to be around 1 mM. Assuming that about 75% of the total pool is phosphorylated, as is the case for Cr, the total Gua pool in the brain would be on the order of 1.3 mM. At this low concentration the signal of Gua may be hard to detect, especially as it occurs at 3.8 ppm in a spectral area with several other overlapping resonances.

In muscle, by using analogous reasoning, Gua levels can be estimated to be ~19 mM, based on an assumed ATP concentration of 8 mM (36) and a phosphorylated fraction of 75%. Despite this high Gua tissue concentration, hardly any signal could be observed at the resonance position of Gua in our in vivo ^{1}H muscle spectra. In cases where a signal for Gua was observed, this signal appeared at best as a broad line. Because the muscle ^{1}H spectra of the GAMT–/– animals were obtained at the magic angle, dipolar interactions cannot account for the large linewidth (19). However, HRMAS spectra of intact muscle of GAMT–/– animals showed a clear singlet for Gua at 3.78 ppm. As HRMAS spectra were obtained at a temperature of 4°C, the difference could possibly be due to conformational or environmental changes in vivo.

Remarkably, the Gua signal appeared to be more distinct in the ^{1}H MR spectra of muscle if a low Cr signal was present, and sometimes very low PCr and high PGua concentrations were observed in the ^{31}P spectrum of muscle. Whether the PGua concentration decreases on increasing PCr concentration should be investigated further using controlled Cr feeding of GAMT–/– animals.

Phosphorylated Guanidinoacetate as a Substitute for Phosphocreatine

The large variation in the amount of PGua and residual PCr observed in GAMT–/– muscle is most likely caused by fluctuations in Cr intake via the food, or fluctuation in cellular import capacity, which in muscle is dependent on the feeding status and presumably other physiological parameters (2).

Based on the observation that CK can play a role in the phosphorylation of Cr analogs (37–39) it is likely that CK activity is the source of PGua in GAMT–/– animals. The utilization of PGua during ischemia was very similar to that of PCr in wt mice (20), despite the fact that the conversion rate may be lower, as shown in brain (13). We do not know, however, if the cytosolic BB-CK in brain and MM-CK in muscle have equal in vivo capacity to convert Gua to PGua. A role of mitochondrial CKs (which also occur at quite different concentrations in muscle and CNS) in this process can be excluded. Study of the utilization of Cr analogs by mitochondrial CKs in (permeabilized) tissue has demonstrated that these isoforms have no role in Gua phosphorylation (37,38).

Comparison With Patient Case Studies

The reduction of (P)Cr in the ^{31}P and ^{1}H MR spectra, and the appearance of PGua in the ^{31}P MR spectra of the brain in our mouse model, revealed a striking similarity to the metabolic findings in human patients (3,4,7–11,13). For muscle, however, only two case studies have been reported so far to our knowledge (10,14). In one case the ^{31}P MR spectrum showed PCr and PGua, as observed in our study in GAMT–/– mice (14). In the other case, however, a large signal at about 0 ppm in the ^{31}P MR spectrum was assigned to PCr (10). No signal for Gua was found in the human ^{1}H MR spectrum (10). As shown in the present study, Gua in muscle gives rise to a broad signal which is hard to detect in vivo even at very low Cr concentrations. Brain MRS in GAMT-deficient patients showed different levels of Cr after oral administration of Cr (3,4,7,9–13). Variable Cr levels were also found in GAMT–/– mice and attributed to differences in oral intake of Cr.

Although different inborn errors of Cr metabolism give rise to a reduction of the Cr signal in MR spectra (40–43), the simultaneous observation of reduced Cr signals and new signals for PGua is highly indicative of GAMT deficiency and can be diagnostically applied.

In summary, our results indicate that Cr synthesis is blocked in GAMT-deficient mice, providing evidence for the existence of only one biosynthetic pathway for Cr production in mammals. We can now use this model for an in-depth study of the effects of oral intake of Cr, the pathophysiological thresholds in the Gua levels in different tissues, and the monitoring of treatment of this disease using MRS.

ACKNOWLEDGMENTS

The authors thank Claudia Soede-Huijbregts for obtaining HRMAS spectra of muscular tissues and Dennis Klomp for fruitful discussions.

REFERENCES

1. Wyss M, Kaddurah-Daouk R. Creatine and creatinine metabolism. Physiol Rev 2000;80:1107–1213.
2. Zhao CR, Shang L, Wang W, Jacobs DO. Myocellular creatine and creatine transporter serine phosphorylation after starvation. J Surg Res 2002;105:10–16.
3. Stöckler S, Holzbach U, Hanefeld F, Marquardt I, Helms G, Requart M, Hanicke W, Frahm J. Creatine deficiency in the brain: a new, treatable inborn error of metabolism. Pediatr Res 1994;36:409–413.
4. Stöckler S, Hanefeld F, Frahm J. Creatine replacement therapy in guanidinoacetate methyltransferase deficiency, a novel inborn error of metabolism. Lancet 1996;348:789–790.
5. Stöckler S, Isbrandt D, Hanefeld F, Schmidt B, von Figura K. Guanidinoacetate methyltransferase deficiency: the first inborn error of creatine metabolism in man. Am J Hum Genet 1996;58:914–922.
6. Stöckler S, Marescau B, De Deyn PP, Trijbels JM, Hanefeld F. Guanidino compounds in guanidinoacetate methyltransferase deficiency, a new inborn error of creatine synthesis. Metabolism 1997;46:1189–1193.
7. Schulze A, Hess T, Wevers R, Mayatepek E, Bachert P, Marescau B, Knopp MV, De Deyn PP, Bremer HJ, Rating D. Creatine deficiency syndrome caused by guanidinoacetate methyltransferase deficiency: diagnostic tools for a new inborn error of metabolism. J Pediatr 1997; 131:626–631.
8. van der Knaap MS, Verhoeven NM, Maaswinkel-Mooij P, Pouwels PJ, Onkenhout W, Peeters EA, Stöckler-Ipsiroglu S, Jakobs C. Mental retardation and behavioral problems as presenting signs of a creatine synthesis defect. Ann Neurol 2000;47:540–543.
9. Ganesan V, Johnson A, Connelly A, Eckhardt S, Surtees RA. Guanidinoacetate methyltransferase deficiency: new clinical features. Pediatr Neurol 1997;17:155–157.
10. Thiel T, Ensenauer R, Hennig J, Lehnert W. In vivo magnetic resonance spectroscopy in a patient with creatine deficiency syndrome: new aspects on mechanism of creatine uptake in brain and muscle. In: Proc 9th Annual Meeting ISMRM, Glasgow, 2001. p 582.
11. Leuzzi V, Bianchi MC, Tosetti M, Carducci C, Cerquiglini CA, Cioni G, Antonozzi I. Brain creatine depletion: guanidinoacetate methyltransferase deficiency (improving with creatine supplementation). Neurology 2000;55:1407–1409.
12. von Figura K, Hanefeld F, Isbrandt D, Stöckler-Ipsiroglu S. Guanidinoacetate methyltransferase deficiency. In: Scriver CR, Beaudet AL, Sly WS, Valle D, Childs B, Vogelstein B, Kinzler KW, editors. The metabolic and molecular bases of inherited disease, 8th ed. New York: McGraw-Hill; 2001. p 1897–1908.
13. Frahm J, Hanefeld F. Localized proton magnetic resonance spectroscopy of brain disorders in childhood. In: Bachelard H, editor. Magnetic resonance spectroscopy and imaging in neurochemistry, vol. 8. Advances in neurochemistry. New York: Plenum Press; 1997. p 329–403.
14. Schulze A, Bachert P, Schlemmer H, Harting I, Polster T, Salomons GS, Verhoeven NM, Jakobs C, Fowler B, Hoffmann GF, Mayatepek E. Lack of creatine in muscle and brain in an adult with GAMT deficiency. Ann Neurol 2003;53:248–251.
15. Isbrandt D, Schmidt A, Neu A, Röper J, Steinfeld R, Ullrich K. Generation of a knockout mouse model for guanidinoacetate methyltransferase (GAMT) deficiency. J Inherit Metab Dis 2002;23(Suppl 1):212.
16. Pfeuffer J, Tkac I, Provencher SW, Gruetter R. Toward an in vivo neurochemical profile: quantification of 18 metabolites in short-echo-time (1)H NMR spectra of the rat brain. J Magn Reson 1999;141:104–120.
17. Ordidge RJ, Connely A, Lohman JAB. Image-selected in vivo spectroscopy (ISIS). A new technique for spatially selective NMR spectroscopy. J Magn Reson 1986;66:293–294.
18. Alderman DW, Grant DM. An efficient decouple coil design which reduces heating in conductive samples in superconducting spectrometers. J Magn Reson 1979;36:447–451.
19. in 't Zandt HJA, Klomp DWJ, Oerlemans F, Wieringa B, Hilbers CW, Heerschap A. Proton MR spectroscopy of wild-type and creatine kinase deficient mouse skeletal muscle: dipole-dipole coupling effects and post-mortem changes. Magn Reson Med 2000;43:517–524.
20. in 't Zandt HJ, Oerlemans F, Wieringa B, Heerschap A. Effects of ischemia on skeletal muscle energy metabolism in mice lacking creatine kinase monitored by in vivo 31P nuclear magnetic resonance spectroscopy. NMR Biomed 1999;12:327–334.

21. Bergmeyer HU. Methods of enzymatic analysis. New York: Academic Press; 1974.
22. Provencher SW. Estimation of metabolite concentrations from localized in vivo proton NMR spectra. Magn Reson Med 1993;30:672–679.
23. http://www.mrui.uab.es/mrui/mruiHomePage.html
24. Sjogaard G, Saltin B. Extra- and intracellular water spaces in muscles of man at rest and with dynamic exercise. Am J Physiol 1982;243:R271–280.
25. Moon RB, Richards JH. Determination of intracellular pH by 31P magnetic resonance. J Biol Chem 1973;248:7276–7278.
26. Torack RM, Alcala H, Gado M, Burton R. Correlative assay of computerized cranial tomography CCT, water content and specific gravity in normal and pathological postmortem brain. J Neuropathol Exp Neurol 1976;35:385–392.
27. Wyss M, Wallimann T. Creatine metabolism and the consequences of creatine depletion in muscle. Mol Cell Biochem 1994;133–134:51–66.
28. Braissant O, Henry H, Loup M, Eilers B, Bachmann C. Endogenous synthesis and transport of creatine in the rat brain: an in situ hybridization study. Brain Res Mol Brain Res 2001;86:193–201.
29. Birken DL, Oldendorf WH. N-acetyl-L-aspartic acid: a literature review of a compound prominent in 1H-NMR spectroscopic studies of brain. Neurosci Biobehav Rev 1989;13:23–31.
30. Hagg T, Van der Zee CEEM, Ross GM, Riopelle RJ. Response to "Petersen et al.: Basal forebrain neuronal loss in mice lacking neurotrophin receptor p75." Science 1997;277:838–839.
31. Cruz F, Cerdan S. Quantitative 13C NMR studies of metabolic compartmentation in the adult mammalian brain. NMR Biomed 1999;12:451–462.
32. Pouwels PJW, Frahm J. Regional metabolite concentrations in human brain as determined by quantitative localized proton MRS. Magn Reson Med 1998;39:53–60.
33. van Pilsum JF, Olsen B, Taylor D, Rozycki T, Pierce JC. Transamidinase activities, in vitro, of tissues from various mammals and from rats fed in protein-free, creatine-supplemented and normal diets. Arch Biochem Biophys 1963;100:520–524.
34. Wyss M, Schulze A. Health implications of creatine: can oral creatine supplementation protect against neurological and atherosclerotic disease? Neuroscience 2002;112:243–260.
35. Gorell JM, Dolkart PH, Ferrendelli JA. Regional levels of glucose, amino acids, high energy phosphates, and cyclic nucleotides in the central nervous system during hypoglycemic stupor and behavioral recovery. J Neurochem 1976;27:1043–1049.
36. van Deursen J, Heerschap A, Oerlemans F, Ruitenbeek W, Jap P, ter Laak H, Wieringa B. Skeletal muscles of mice deficient in muscle creatine kinase lack burst activity. Cell 1993;74:621–631.
37. van Deursen J, Jap P, Heerschap A, ter Laak H, Ruitenbeek W, Wieringa B. Effects of the creatine analogue beta-guanidinopropionic acid on skeletal muscles of mice deficient in muscle creatine kinase. Biochim Biophys Acta 1994;1185:327–335.
38. Boehm EA, Radda GK, Tomlin H, Clark JF. The utilisation of creatine and its analogues by cytosolic and mitochondrial creatine kinase. Biochim Biophys Acta 1996;1274:119–128.
39. Holtzman D, McFarland E, Moerland T, Koutcher J, Kushmerick MJ, Neuringer LJ. Brain creatine phosphate and creatine kinase in mice fed an analogue of creatine. Brain Res 1989;483:68–77.
40. de Grauw TJ, Cecil KC, Salomons GS, van Doornen SJM, Verhoeven NM, Ball WS, Jakobs C. The clinical syndrome of creatine transporter deficiency. In: Abstracts 6th Int Conf Guanidino Comp Biology Med, Cincinnati, 2001.
41. Cecil KM, Salomons GS, Ball Jr WS, Wong B, Chuck G, Verhoeven NM, Jakobs C, DeGrauw TJ. Irreversible brain creatine deficiency with elevated serum and urine creatine: a creatine transporter defect? Ann Neurol 2001;49:401–404.
42. Bianchi MC, Tosetti M, Fornai F, Alessandri MG, Cipriani P, De Vito G, Canapicchi R. Reversible brain creatine deficiency in two sisters with normal blood creatine level. Ann Neurol 2000;47:511–513.
43. Item CB, Stockler-Ipsiroglu S, Stromberger C, Muhl A, Alessandri MG, Bianchi MC, Tosetti M, Fornai F, Cioni G. Arginine:glycine amidinotransferase deficiency: the third inborn error of creatine metabolism in humans. Am J Hum Genet 2001;69:1127–1133.